

Potential Genes and Pathways Associated with Heterotopic Ossification, Derived from Analyses of Gene Expression Profiles

Zhanyu Yang (✉ doctoryangzhanyu@163.com)

Hunan Provincial People's Hospital <https://orcid.org/0000-0001-8820-5710>

Delong Liu

Hunan Provincial People's Hospital

Rui Guan

Hunan Provincial People's Hospital

Xin Li

Hunan Provincial People's Hospital

Yiwei Wang

Hunan Provincial People's Hospital

Bin Sheng

Hunan Provincial People's Hospital

Research Article

Keywords: heterotopic ossification, bioinformatic analysis, differentially expressed genes, protein-protein interaction, functional enrichment analysis

Posted Date: June 4th, 2021

DOI: <https://doi.org/10.21203/rs.3.rs-572774/v1>

License:   This work is licensed under a Creative Commons Attribution 4.0 International License.

[Read Full License](#)

Version of Record: A version of this preprint was published at Journal of Orthopaedic Surgery and Research on August 14th, 2021. See the published version at <https://doi.org/10.1186/s13018-021-02658-1>.

Abstract

Background: Heterotopic ossification (HO) represents pathological lesions, referred to the development of heterotopic bone in extraskkeletal tissues around joints. This study will investigate the genetic characteristics of bone marrow mesenchymal stem cells (BMSCs) from HO tissues and explore the potential pathways involved.

Methods: The gene expression profiles (GSE94683) was obtained from the Gene Expression Omnibus (GEO), including 9 normal specimens and 7 HO specimens, and differentially expressed genes (DEGs) were identified. Then, the protein-protein interaction (PPI) networks, Gene Ontology (GO) and Kyoto Encyclopaedia of Genes and Genomes (KEGG) enrichment analysis were performed for further analysis.

Results: Totally 275 DEGs were differentially expressed, of which 153 were upregulated and 122 were downregulated. In the biological process (BP), the majority of DEGs, including EFNB3, UNC5C, TMEFF2, PTH2, KIT, FGF13 and WISP3, were intensively enriched in cell signal transmission items, including axon guidance, negative regulation of cell migration, peptidyl-tyrosine phosphorylation and cell-cell signaling. Moreover, KEGG analysis indicated that the majority of DEGs, including EFNB3, UNC5C, FGF13, MAPK10, DDIT3, KIT, COL4A4 and DKK2, primarily involved in mitogen-activated protein kinase (MAPK) signaling pathway, Ras signaling pathway, phosphatidylinositol-3-kinase/protein kinase B (PI3K/Akt) signaling pathway and Wnt signaling pathway. 10 hub genes were identified, including CX3CL1, CXCL1, ADAMTS3, ADAMTS16, ADAMTSL2, ADAMTSL3, ADAMTSL5, PENK, GPR18, CALB2.

Conclusions: This study presents a novel insight into the pathogenesis of HO. 10 hub genes and most of the DEGs intensively involved in enrichment analyses may be the new candidate targets for the prevention and treatment of HO in the future.

Background

Heterotopic ossification (HO) represents pathological lesions, referred to the development of heterotopic bone in extraskkeletal tissues around joints, which often occurs in the elbow, thigh, pelvis, and shoulder.(1, 2) The clinical manifestations were altered with the progression of the disease. Local pain, tenderness, swelling and stiffness of the involved joints were presented in the early stage of HO. At the end of the disease, it even presents with complete ankyloses, which seriously damages the quality of life.(3) The specific causes of HO were still uncertain. It is generally believed that the occurrence is related to genetic susceptibility and severe trauma. Progressive ossifying fibrous dysplasia (FOP), a genetic hereditary form of HO, is extremely rare with the prevalence of about 1:2000000 in the population.(4–7) However, there was a much higher incidence of HO following soft-tissue trauma, amputations, central nervous system injury, such as cerebral anoxia, encephalitis, traumatic brain injuries and spinal cord lesions.(8, 9)

At present, the only effective way to treat HO is surgical resection of ossified tissue. Since HO is prone to recurrence, this method is only temporarily effective.(10) Moreover, when the ossification tissue invades the large blood vessels and nerves, the complication rate caused by resection is also increased. Studies

have shown that HO is a disease with unknown pathogenesis, inadequate prevention and treatment, and high disability rate.(11) Therefore, in order to find a more effective therapeutic method, we need to better understand the pathogenesis of HO.(12)

Recently, the bioinformatics analysis of gene expression, which served as a key technology in mechanism exploration, play an important role in screening gene mutations and studying genetic behavior. Our study screened out the genes differentially expressed in bone marrow mesenchymal stem cells (BMSCs) from HO, which were identified from a public dataset. In this work, we seek to synthesize the protein-protein interaction (PPI) networks analysis, Gene Ontology (GO) and Kyoto Encyclopaedia of Genes and Genomes (KEGG) enrichment analysis among DEGs to explore the potential mechanism of HO and candidate gene targets, which may be used to prevent, alleviate and even reverse the progress of HO.

Methods

Microarray data resource

A gene expression profile dataset (GSE94683),

The GSE94683,(13) a gene expression profile dataset obtained from a public genomics data repository (GEO database, <http://www.ncbi.nlm.nih.gov/geo/>), was produced on the GPL10630 Agilent-021531 Whole Human Genome Oligo Microarray 4x44K. According to the annotation information in the platform, the probes were alternated into corresponding gene symbols. GSE94683 contains 9 normal specimens and 7 HO specimens. HO specimens were obtained from patients with injuries at Garches Hospital, Garches, France. Healthy specimens were obtained from patients after total hip surgery at Blois Hospital (Blois, France) and at Centre de Transfusion Sanguine des Armées (Percy Hospital, Clamart, France).

Data processing and Identification of DEGs

Principal components analysis (PCA) and the normalization were performed by ggbiplot and the preprocessCore package in R. After the preprocessing of the datasets, the identification of DEGs were processed using Multiple Linear Regression Models via limma package of R language. A probe without any corresponding gene symbol was eliminated and a gene with a plenty of probes was averaged. All DEGs and top 30 DEGs were demonstrated via volcano plot, which was performed by ggplot2 package. DEGs were screened by using classical *t* test and $|\text{Log}_2(\text{FoldChange})| > 2$ and $\text{adj. } P < 0.05$ was defined as a threshold and criteria for identification of statistically significant DEGs. The relative expression values of total DEGs and top 30 upregulated and downregulated DEGs, which were extracted from gene expression profile, were demonstrated by the hierarchical clustering heatmaps via pheatmap package of R language.

Functional enrichment analysis for DEGs

KEGG is a data reservoir for unravelling advanced biological functions and pathways involved with genomic information.(14) GO is a tool for defining concepts or classifying gene biological function by

analyzing a large list of genes.(15) The Database for Annotation, Visualization and Integrated Discovery (DAVID), a web-based database resource that explores gene data, facilitates researchers to reveal the potential genetic significance.(16) The DAVID performed the GO and KEGG enrichment analyses. The functional enrichment analyses were processed via ggplot2 package in R and demonstrated by the bubble plots.

Integration of PPI network analysis

Search Tool for the Retrieval of Interacting Genes (STRING), an original online program that predicts the relationships and interactions among proteins involved,(17) was applied to construct functional network among proteins. Cytoscape, an open-accessed visual tool, was able to visualize processes and interactions among proteins. Molecular Complex Detection (MCODE), a plugin of Cytoscape, was used to explore intensively communications and discover the most significant module. "MCODE scores ≥ 5 ", "k-score = 2", "Max depth = 100", "node score cut-off = 0.2" and "degree cut-off = 2" were selected as criterion for identification of significant modules.

Hub genes selection and analyses

CytoHubba, a plugin of Cytoscape applied with 12 topological analysis methods, was used to detect more comprehensive hub genes and avoid missing. According to MCC, MNC, DMNC and Degree, the top 25 genes were predicted. Venn diagrams were used to screen the hub genes by identifying the overlapping genes.

Results

Data source and data preprocessing

As large amounts of data were integrated in a gene expression profile (GSE94683), the original data was downloaded from GEO database. PCA of datasets demonstrated that there were significant differences between HO samples and control samples (Fig. 1). Normalization of the data was presented in a boxplot (Fig. 2).

DEGs in HO samples compared with control samples

A total of 275 DEGs were identified on the basis of the criteria established, including 122 downregulated genes and 153 upregulated genes. The expression level of total and top 30 DEGs were shown in volcano plots and heatmap (Fig. 3 and Fig. 4), indicating that the expression level of DEGs could effectively differentiate the two groups.

Functional enrichment analysis for DEGs

DAVID was used to perform functional enrichment analyses to explore the biological classification of DEGs and the top 10 items were shown in Fig. 5. In the biological process (BP) ontology, the majority of

DEGs, including EFNB3, UNC5C, TMEFF2, PTH2, KIT, FGF13 and WISP3 were intensively enriched in cell signal transmission items, including axon guidance (9 genes), negative regulation of cell migration (7 genes), peptidyl-tyrosine phosphorylation (6 genes) and cell-cell signaling (10 genes). Moreover, KEGG analysis indicated that the majority of DEGs, including EFNB3, UNC5C, FGF13, MAPK10, DDIT3, KIT, COL4A4 and DKK2, primarily involved in axon guidance (7 genes), mitogen-activated protein kinase (MAPK) signaling pathway (9 genes), Ras signaling pathway (7 genes), phosphatidylinositol-3-kinase/protein kinase B (PI3K/Akt) signaling pathway (9 genes) and Wnt signaling pathway (5 genes).

PPI network construction and hub gene selection

The PPI network has been constructed after the data of the functional relationships and interactions obtained from the STRING were imported into the Cytoscape, and the top module was identified (Fig. 6). According to MCC, MNC, DMNC and Degree, the top 25 genes (10%) were predicted. Venn diagrams were used to select the hub genes, and CX3CL1, CXCL1, ADAMTS3, ADAMTS16, ADAMTSL2, ADAMTSL3, ADAMTSL5, PENK, GPR18, CALB2, were identified as the hub genes (Fig. 7).

Discussion

HO refers to a pathological process, involving a variety of etiology, location, mechanism and cell origin.(3) It is reported that early diagnosis of HO is difficult due to lack of evident signs and symptoms and limited treatment.(18, 19) How to manipulate the inflammatory cascades to control HO formation is just beginning to be understood.(3) Therefore, it is urgent to explore the mechanisms of the formation of HO at the molecular level, so as to find novel, adequate and effective treatment methods to alleviate, delay, or even reverse the development of HO.

The whole-genome microarray and bioinformatic analysis facilitate us to detect genetic differences in the development of HO, and provide a better way to explore the pathogenesis and identify novel candidates for early diagnosis and precise treatment. In current study, 275 DEGs were identified, including 122 downregulated genes and 153 upregulated genes.

After that, the functional enrichment analysis was performed, and the relationships and interactions among DEGs were predicted. The majority of DEGs, including KIT, FGF13, EFNB3, UNC5C, TMEFF2, WISP3 and PTH2 were intensively enriched in cell signal transmission items, including axon guidance, negative regulation of cell migration, peptidyl-tyrosine phosphorylation and cell-cell signaling. Moreover, KEGG analysis indicated that the majority of DEGs, including KIT, DDIT3, FGF13, EFNB3, UNC5C, MAPK10 and DKK2, primarily involved in axon guidance, MAPK signaling pathway, Ras signaling pathway, PI3K-Akt signaling pathway and Wnt signaling pathway. This is consistent with the recent research findings that muscle-derived mesenchymal stem cells in the soft tissue migrate to the area of trauma and inflammation, differentiate into osteoblasts and form heterotopic bone.(20)

The PPI network of the DEGs has been constructed. The results indicates that CX3CL1, CXCL1, ADAMTS3, ADAMTS16, ADAMTSL2, ADAMTSL3, ADAMTSL5, PENK, GPR18, CALB2 are hub genes.

Chemokines are able to mediate the migration and localization of immunocyte in the process of inflammation, which plays a vital role in manipulating the immune system. According to the conserved cysteine motifs, chemokines in mankind are divided into four families (C, CC, CXC, and CX3C). Most chemokines are involved in the differentiation of osteoblasts and/or osteoclasts to varying degrees. CX3CL1, belonging to the CX3C subgroup, is a combination of the properties of chemotactic agents and adhesion molecules, which has been shown to continuously control reshaping bone matrix by regulating bone remodeling at the cellular level.(21, 22) Current studies have reported that osteoblasts are able to express CX3CL1, and osteoclast progenitors are able to produce CX3C receptor 1 (CX3CR1).(23) Cytokines originated from inflammation are able to significantly induce the expression of CX3CL1 in osteoblasts. Meanwhile, CX3CR1 are identified as a candidate for screening osteoclasts with inflammatory reaction.(24–26) It was reported that the interaction between membrane-bound CX3CL1 on osteoblasts and CX3CR1 expressed by osteoclast progenitors is able to promote the progress of terminal differentiation of osteoclast progenitors.(23) CX3CR1-deficient mice showed moderate but significantly increased trabecular bone mass, which was mainly due to the decrease in the number of osteoclasts.(27) In vitro experiments suggested that this phenotype can be explained by the decreased ratio of receptor activator of nuclear factor-kappa B ligand/osteoprotegerin (RANKL/OPG), and the defect of spontaneous-formation of osteoclasts from CX3CR1-deficient bone marrow cells.(27) In general, it indicates that CX3CL1 may be involved in osteoclast-mediated bone loss. CXCL1, belonging to the CXC subgroup, is a kind of growth factors that could send signals through CXC receptor 2 (CXCR2).(28) CXCR2, a G protein-coupled receptor, is found remarkably expressed in osteoclast precursors, while it cannot be detected in the osteoblast lineage predominantly. Cell culture studies have confirmed that recombinant CXCL1 is able to stimulate the migration of osteoclast precursors in a dose-dependent manner.(29) Moreover, CXCL1 has been proven to promote osteoclast formation in vitro.(30)

The superfamily of ADAM metalloproteinase with thrombospondin type 1 motif (ADAMTS) comprises 19 distinct ADAMTS, which are consist of secreted enzymes and seven ADAMTS-like proteins (ADAMTSLs) without enzymatic activity.(31–33) Most of them are involved in the generation and degradation of extracellular matrix (ECM) molecules, and participate in the formation and remodeling of connective tissue and the occurrence and development of diseases.(32, 34) The ECM of normal cartilage maintains a dynamic balance between generation and degradation, which is in a state of equilibrium. There is a loss of balance between the proteases and their inhibitors that degrade the ECM in pathological cartilage. ADAMTS3 has been proven to be involved in the formation of type II fibrous collagen in articular cartilage.(35) ADAMTS16, there is no known specific function for articular cartilage yet. Current studies have shown that the expression of ADAMTS16 is increased in cartilage and synovium from osteoarthritis patients compared with the normal.(36, 37) The steady increase of expression of ADAMTS16 will cause the inhibition of cell proliferation, migration and adhesion, and a decreased expression of matrix metalloproteinase-13 (MMP13) in chondrosarcoma cells.(38) Studies have indicated that ADAMTSLs possess specific extracellular ligands and several of them are ECM-binding proteins that act at the cell-matrix interface.(39–41) It is well known that fibrillin microfibrils are able to bind to ADAMTSLs.(42–45)

Therefore, ADAMTSLs can be regarded as matricellular proteins, which are a kind of non-structural proteins expressed in ECM dynamically and with regulatory effects.

PENK, a classically identified opioid gene, was initially shown to be expressed almost exclusively in the mature nervous and neuroendocrine systems. Current studies have revealed that the expression of PENK is selectively increased in mineralized cultures, and it is essential for the formation and remodeling of bone structure.(46) The expression of PENK in osteoblasts is regulated by bone-targeting hormones, which makes a valuable contribution toward bone development.(47)

The interaction among bone formation and hub genes GPR18 and CALB2 have not been reported yet. GPR18 is a receptor for endocannabinoid N-arachidonyl glycine (NAGly).(48, 49) GPR18 may be involved in the regulation of immune system, whose activity is mediated by G proteins that can inhibit adenylyl cyclase.(48) CALB2, a member of the troponin C superfamily, is an intracellular calcium-binding protein and is abundant in auditory neurons and functions as a modulator of neuronal excitability.

Conclusions

In summary, the current study aims to determine potential biomarkers that might be related to the development of HO and to explore the potential mechanism of HO. Totally, 275 DEGs and 8 hub genes were identified, which provided a new promising perspective for HO diagnosis and treatment. However, the biological functions of these biomarkers in the pathogenesis of HO need to be further studied.

Abbreviations

HO = Heterotopic ossification, BMSCs = Bone marrow mesenchymal stem cells, GEO = Gene Expression Omnibus, DEGs = Differentially expressed genes, PPI = Protein-protein interaction, STRING = Search Tool for the Retrieval of Interacting Genes, GO = Gene Ontology, KEGG = Kyoto Encyclopaedia of Genes and Genomes, BP = Biological process, EFNB3 = Ephrin B3, UNC5C = Unc-5 netrin receptor C, TMEFF2 = Transmembrane protein with EGF like and two follistatin like domains 2, PTH2 = Parathyroid hormone 2, KIT = Mast/stem cell growth factor receptor Kit, FGF13 = Fibroblast growth factor 13, WISP3 = WNT1 inducible signaling pathway, MAPK10 = Mitogen-activated protein kinase 10, DDIT3 = DNA damage inducible transcript 3, COL4A4 = Collagen type IV alpha 4 chain, DKK2 = Dickkopf WNT signaling pathway inhibitor 2, MAPK = Mitogen-activated protein kinase, PI3K/Akt = Phosphatidylinositol-3-kinase/protein kinase B, CX3CL1 = C-X3-C motif chemokine ligand 1, CXCL1 = C-X-C motif chemokine ligand 1, ADAMTS = ADAM metalloproteinase with thrombospondin type 1 motif, ADAMTSLs = ADAMTS-like proteins, PENK = Proenkephalin, GPR18 = G protein-coupled receptor 18, CALB2 = Calbindin 2, FOP = Progressive ossifying fibrous dysplasia, PCA = Principal components analysis, DAVID = Database for Annotation, Visualization and Integrated Discovery, MCODE = Molecular Complex Detection, CX3CR1 = CX3C receptor 1, CXCR2 = CXC receptor 2, RANKL/OPG = Receptor activator of nuclear factor-kappa B ligand/osteoprotegerin, ECM = Extracellular matrix, MMP13 = Matrix metalloproteinase 13, NAGly = N-arachidonyl glycine.

Declarations

Ethics approval and consent to participate

This article does not contain any studies with human participants or animals performed by any of the authors.

Consent for publication

Not applicable.

Availability of data and materials

All data generated or analyzed during this study are included in published articles.

Competing interests

All authors declare they have no conflicts of interest or competing interests.

Funding

This research did not receive any specific grant from funding agencies in the public, commercial, or not-for-profit sectors.

Authors' contributions

YZY and SB conceived and designed the study. YZY, LDL and LX analyzed the data and wrote the manuscript. The original text was drafted and modified by GR and WYW. All authors read and approved the final manuscript.

Acknowledgements

Not applicable.

References

1. Hoch B, Montag A. Reactive bone lesions mimicking neoplasms. *Semin Diagn Pathol.* 2011;28(1):102–12.
2. Mavrogenis AF, Soucacos PN, Papagelopoulos PJ. Heterotopic ossification revisited. *Orthopedics.* 2011;34(3):177.
3. Meyers C, Lisiecki J, Miller S, Levin A, Fayad L, Ding C, et al. Heterotopic Ossification: A Comprehensive Review. *JBMR plus.* 2019;3(4):e10172.
4. van Dinther M, Visser N, de Gorter DJ, Doorn J, Goumans MJ, de Boer J, et al. ALK2 R206H mutation linked to fibrodysplasia ossificans progressiva confers constitutive activity to the BMP type I receptor

- and sensitizes mesenchymal cells to BMP-induced osteoblast differentiation and bone formation. *Journal of bone mineral research: the official journal of the American Society for Bone Mineral Research*. 2010;25(6):1208–15.
5. Shore EM, Xu M, Feldman GJ, Fenstermacher DA, Cho TJ, Choi IH, et al. A recurrent mutation in the BMP type I receptor ACVR1 causes inherited and sporadic fibrodysplasia ossificans progressiva. *Nat Genet*. 2006;38(5):525–7.
 6. Fukuda T, Kohda M, Kanomata K, Nojima J, Nakamura A, Kamizono J, et al. Constitutively activated ALK2 and increased SMAD1/5 cooperatively induce bone morphogenetic protein signaling in fibrodysplasia ossificans progressiva. *J Biol Chem*. 2009;284(11):7149–56.
 7. Chakkalakal SA, Zhang D, Culbert AL, Convente MR, Caron RJ, Wright AC, et al. An Acvr1 R206H knock-in mouse has fibrodysplasia ossificans progressiva. *Journal of bone mineral research: the official journal of the American Society for Bone Mineral Research*. 2012;27(8):1746–56.
 8. Sakellariou VI, Grigoriou E, Mavrogenis AF, Soucacos PN, Papagelopoulos PJ. Heterotopic ossification following traumatic brain injury and spinal cord injury: insight into the etiology and pathophysiology. *J Musculoskel Neuronal Interact*. 2012;12(4):230–40.
 9. Seipel R, Langner S, Platz T, Lippa M, Kuehn JP, Hosten N. Neurogenic heterotopic ossification: epidemiology and morphology on conventional radiographs in an early neurological rehabilitation population. *Skeletal Radiol*. 2012;41(1):61–6.
 10. Genet F, Chehensse C, Jourdan C, Lautridou C, Denormandie P, Schnitzler A. Impact of the operative delay and the degree of neurologic sequelae on recurrence of excised heterotopic ossification in patients with traumatic brain injury. *J Head Trauma Rehabil*. 2012;27(6):443–8.
 11. Xu JC, Wu GH, Zhou LL, Yang XJ, Liu JT. Establishment of heterotopic ossification via sharp instrument injury in rats. *J Musculoskel Neuronal Interact*. 2017;17(1):456–60.
 12. Brady RD, Shultz SR, McDonald SJ, O'Brien TJ. Neurological heterotopic ossification: Current understanding and future directions. *Bone*. 2018;109:35–42.
 13. Torossian F, Guerton B, Anginot A, Alexander KA, Desterke C, Soave S, et al. Macrophage-derived oncostatin M contributes to human and mouse neurogenic heterotopic ossifications. *JCI insight*. 2017;2:21.
 14. Kanehisa M, Goto S. KEGG: kyoto encyclopedia of genes and genomes. *Nucleic acids research*. 2000;28(1):27–30.
 15. The Gene Ontology (GO). project in 2006. *Nucleic acids research*. 2006;34(Database issue):D322-6.
 16. Dennis G Jr, Sherman BT, Hosack DA, Yang J, Gao W, Lane HC, et al. DAVID: Database for Annotation, Visualization, and Integrated Discovery. *Genome biology*. 2003;4(5):P3.
 17. Szklarczyk D, Franceschini A, Wyder S, Forslund K, Heller D, Huerta-Cepas J, et al. STRING v10: protein-protein interaction networks, integrated over the tree of life. *Nucleic acids research*. 2015;43(Database issue):D447-52.
 18. Agarwal S, Loder S, Brownley C, Cholok D, Mangiavini L, Li J, et al. Inhibition of Hif1alpha prevents both trauma-induced and genetic heterotopic ossification. *Proc Natl Acad Sci USA*.

- 2016;113(3):E338-47.
19. Choi YH, Kim KE, Lim SH, Lim JY. Early presentation of heterotopic ossification mimicking pyomyositis - two case reports. *Annals of rehabilitation medicine*. 2012;36(5):713–8.
 20. Molligan J, Mitchell R, Schon L, Achilefu S, Zahoor T, Cho Y, et al. Influence of Bone and Muscle Injuries on the Osteogenic Potential of Muscle Progenitors: Contribution of Tissue Environment to Heterotopic Ossification. *Stem cells translational medicine*. 2016;5(6):745–53.
 21. Niedzwiedzki T, Filipowska J. Bone remodeling in the context of cellular and systemic regulation: the role of osteocytes and the nervous system. *J Mol Endocrinol*. 2015;55(2):R23–36.
 22. Brylka LJ, Schinke T. Chemokines in Physiological and Pathological Bone Remodeling. *Frontiers in immunology*. 2019;10:2182.
 23. Koizumi K, Saitoh Y, Minami T, Takeno N, Tsuneyama K, Miyahara T, et al. Role of CX3CL1/fractalkine in osteoclast differentiation and bone resorption. *Journal of immunology (Baltimore, Md: 1950)*. 2009;183(12):7825-31.
 24. Isozaki T, Kasama T, Takahashi R, Odai T, Wakabayashi K, Kanemitsu H, et al. Synergistic induction of CX3CL1 by TNF alpha and IFN gamma in osteoblasts from rheumatoid arthritis: involvement of NF-kappa B and STAT-1 signaling pathways. *Journal of inflammation research*. 2008;1:19–28.
 25. Matsuura T, Ichinose S, Akiyama M, Kasahara Y, Tachikawa N, Nakahama KI. Involvement of CX3CL1 in the Migration of Osteoclast Precursors Across Osteoblast Layer Stimulated by Interleukin-1ss. *Journal of cellular physiology*. 2017;232(7):1739–45.
 26. Ibanez L, Abou-Ezzi G, Ciucci T, Amiot V, Belaid N, Obino D, et al. Inflammatory Osteoclasts Prime TNFalpha-Producing CD4(+) T Cells and Express CX3 CR1. *Journal of bone mineral research: the official journal of the American Society for Bone Mineral Research*. 2016;31(10):1899–908.
 27. Hoshino A, Ueha S, Hanada S, Imai T, Ito M, Yamamoto K, et al. Roles of chemokine receptor CX3CR1 in maintaining murine bone homeostasis through the regulation of both osteoblasts and osteoclasts. *Journal of cell science*. 2013;126(Pt 4):1032–45.
 28. Lee YC, Gajdosik MS, Josic D, Clifton JG, Logothetis C, Yu-Lee LY, et al. Secretome analysis of an osteogenic prostate tumor identifies complex signaling networks mediating cross-talk of cancer and stromal cells within the tumor microenvironment. *Molecular cellular proteomics: MCP*. 2015;14(3):471–83.
 29. Onan D, Allan EH, Quinn JM, Gooi JH, Pompolo S, Sims NA, et al. The chemokine Cxcl1 is a novel target gene of parathyroid hormone (PTH)/PTH-related protein in committed osteoblasts. *Endocrinology*. 2009;150(5):2244–53.
 30. Hardaway AL, Herroon MK, Rajagurubandara E, Podgorski I. Marrow adipocyte-derived CXCL1 and CXCL2 contribute to osteolysis in metastatic prostate cancer. *Clin Exp Metastasis*. 2015;32(4):353–68.
 31. Kuno K, Kanada N, Nakashima E, Fujiki F, Ichimura F, Matsushima K. Molecular cloning of a gene encoding a new type of metalloproteinase-disintegrin family protein with thrombospondin motifs as an inflammation associated gene. *J Biol Chem*. 1997;272(1):556–62.

32. Apte SS. A disintegrin-like and metalloprotease (reprolysin-type) with thrombospondin type 1 motif (ADAMTS) superfamily: functions and mechanisms. *J Biol Chem.* 2009;284(46):31493–7.
33. Apte SS. A disintegrin-like and metalloprotease (reprolysin type) with thrombospondin type 1 motifs: the ADAMTS family. *Int J Biochem Cell Biol.* 2004;36(6):981–5.
34. Dubail J, Apte SS. Insights on ADAMTS proteases and ADAMTS-like proteins from mammalian genetics. *Matrix biology: journal of the International Society for Matrix Biology.* 2015;44–46:24–37.
35. Fernandes RJ, Hirohata S, Engle JM, Colige A, Cohn DH, Eyre DR, et al. Procollagen II amino propeptide processing by ADAMTS-3. Insights on dermatosparaxis. *J Biol Chem.* 2001;276(34):31502–9.
36. Kevorkian L, Young DA, Darrah C, Donell ST, Shepstone L, Porter S, et al. Expression profiling of metalloproteinases and their inhibitors in cartilage. *Arthritis rheumatism.* 2004;50(1):131–41.
37. Davidson RK, Waters JG, Kevorkian L, Darrah C, Cooper A, Donell ST, et al. Expression profiling of metalloproteinases and their inhibitors in synovium and cartilage. *Arthritis research therapy.* 2006;8(4):R124.
38. SurrIDGE AK, Rodgers UR, Swingler TE, Davidson RK, Kevorkian L, Norton R, et al. Characterization and regulation of ADAMTS-16. *Matrix biology: journal of the International Society for Matrix Biology.* 2009;28(7):416–24.
39. Hirohata S, Wang LW, Miyagi M, Yan L, Seldin MF, Keene DR, et al. Punctin, a novel ADAMTS-like molecule, ADAMTSL-1, in extracellular matrix. *J Biol Chem.* 2002;277(14):12182–9.
40. Hall NG, Klenotic P, Anand-Apte B, Apte SS. ADAMTSL-3/punctin-2, a novel glycoprotein in extracellular matrix related to the ADAMTS family of metalloproteases. *Matrix biology: journal of the International Society for Matrix Biology.* 2003;22(6):501–10.
41. Koo BH, Le Goff C, Jungers KA, Vasanthi A, O'Flaherty J, Weyman CM, et al. ADAMTS-like 2 (ADAMTSL2) is a secreted glycoprotein that is widely expressed during mouse embryogenesis and is regulated during skeletal myogenesis. *Matrix biology: journal of the International Society for Matrix Biology.* 2007;26(6):431–41.
42. Le Goff C, Mahaut C, Wang LW, Allali S, Abhyankar A, Jensen S, et al. Mutations in the TGFbeta binding-protein-like domain 5 of FBN1 are responsible for acromicric and geleophysic dysplasias. *Am J Hum Genet.* 2011;89(1):7–14.
43. Gabriel LA, Wang LW, Bader H, Ho JC, Majors AK, Hollyfield JG, et al. ADAMTSL4, a secreted glycoprotein widely distributed in the eye, binds fibrillin-1 microfibrils and accelerates microfibril biogenesis. *Investig Ophthalmol Vis Sci.* 2012;53(1):461–9.
44. Bader HL, Wang LW, Ho JC, Tran T, Holden P, Fitzgerald J, et al. A disintegrin-like and metalloprotease domain containing thrombospondin type 1 motif-like 5 (ADAMTSL5) is a novel fibrillin-1-, fibrillin-2-, and heparin-binding member of the ADAMTS superfamily containing a netrin-like module. *Matrix biology: journal of the International Society for Matrix Biology.* 2012;31(7–8):398–411.
45. Tsutsui K, Manabe R, Yamada T, Nakano I, Oguri Y, Keene DR, et al. ADAMTSL-6 is a novel extracellular matrix protein that binds to fibrillin-1 and promotes fibrillin-1 fibril formation. *J Biol*

Chem. 2010;285(7):4870–82.

46. Seitz S, Barvencik F, Gebauer M, Albers J, Schulze J, Streichert T, et al. Preproenkephalin (Penk) is expressed in differentiated osteoblasts, and its deletion in Hyp mice partially rescues their bone mineralization defect. *Calcif Tissue Int.* 2010;86(4):282–93.
47. Rosen H, Krichevsky A, Polakiewicz RD, Benzakine S, Bar-Shavit Z. Developmental regulation of proenkephalin gene expression in osteoblasts. *Molecular endocrinology (Baltimore Md).* 1995;9(11):1621–31.
48. Kohno M, Hasegawa H, Inoue A, Muraoka M, Miyazaki T, Oka K, et al. Identification of N-arachidonylglycine as the endogenous ligand for orphan G-protein-coupled receptor GPR18. *Biochemical and biophysical research communications.* 2006;347(3):827–32.
49. Flegel C, Vogel F, Hofreuter A, Wojcik S, Schoeder C, Kiec-Kononowicz K, et al. Characterization of non-olfactory GPCRs in human sperm with a focus on GPR18. *Scientific reports.* 2016;6:32255.

Figures

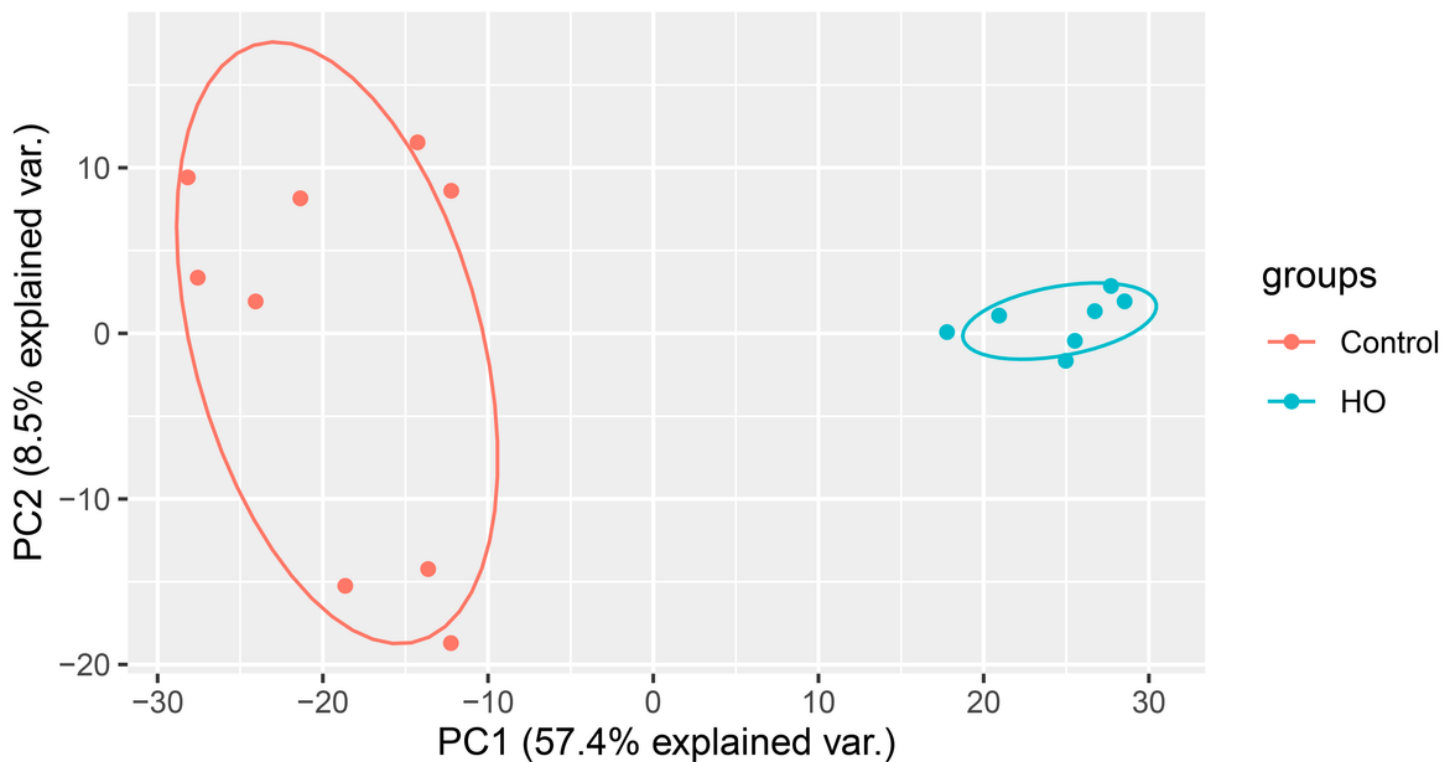


Figure 1

Principal components analysis of datasets. Red represents samples from normal cohort. Blue represents samples from heterotopic ossification.

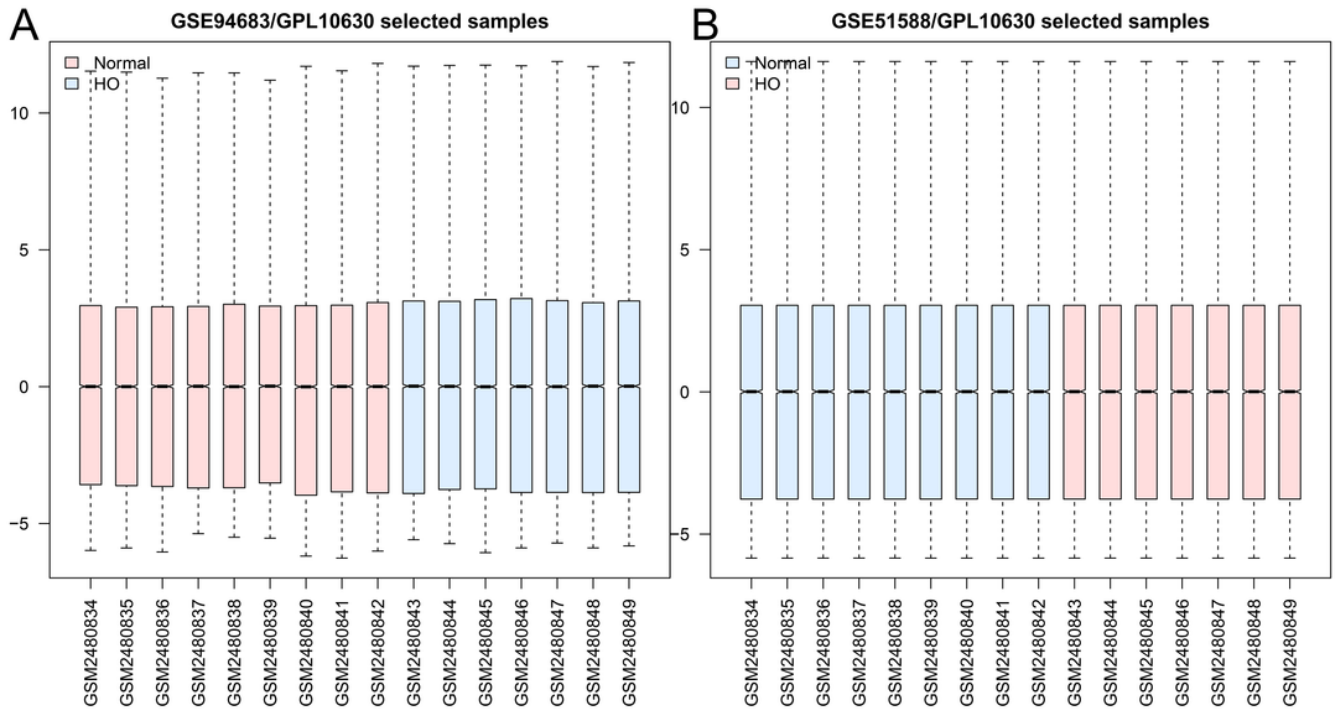


Figure 2

Normalization of the sample data demonstrated by box plot. (A) before processing and (B) after processing. HO = heterotopic ossification, DEGs = differentially expressed genes.

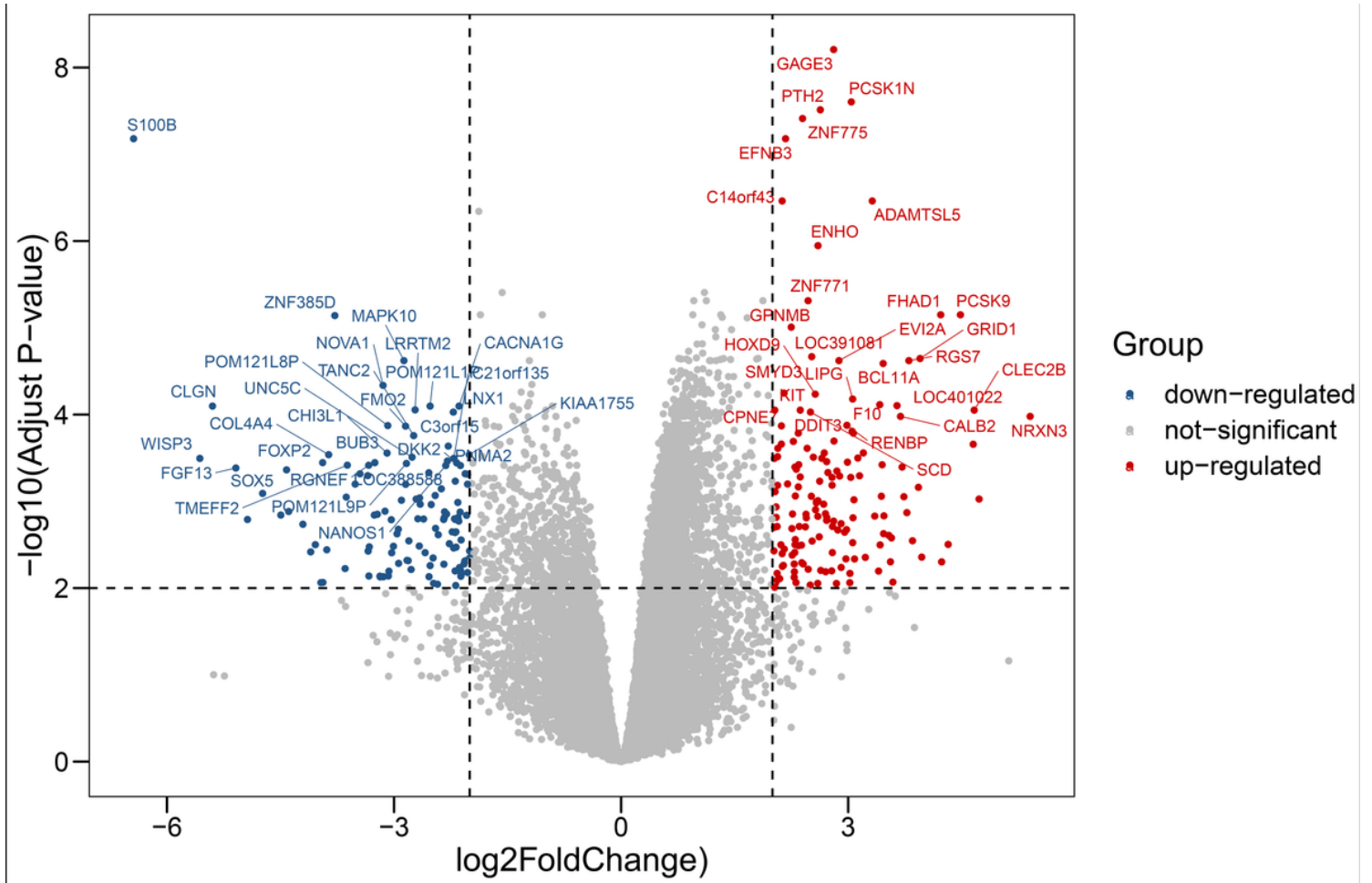


Figure 3

DEGs screening identified by volcano plot. Grey refers to no difference in expression. Red refers to up-regulated expression. Blue refers to down-regulated expression.

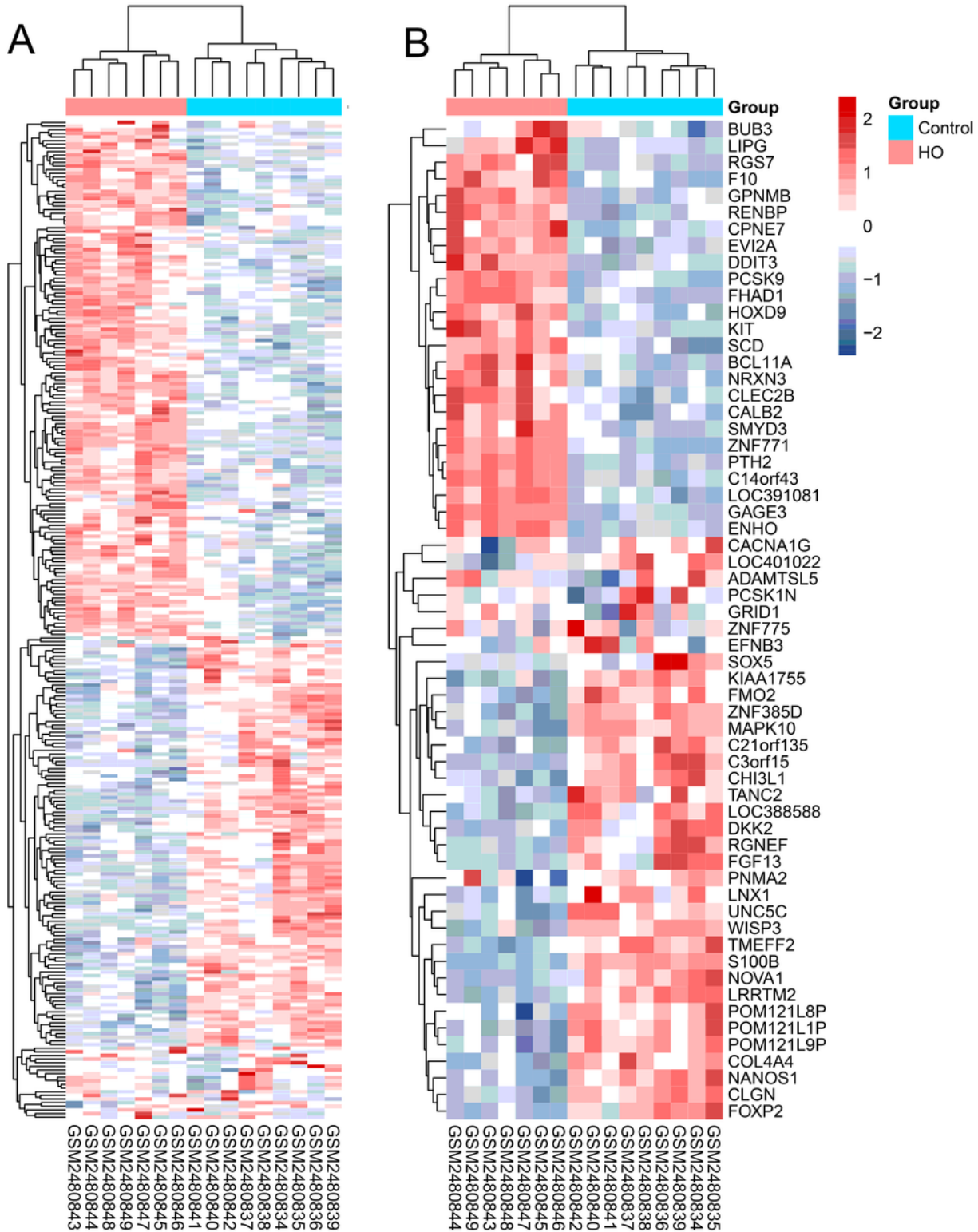


Figure 4

DEGs in expression demonstrated via heatmap. (A) total DEGs and (B) top 30 DEGs. Red refers to up-regulated expression. Blue refers to down-regulated expression. Max = maximum, min = minimum, BMCs = bone marrow mesenchymal stem cells.

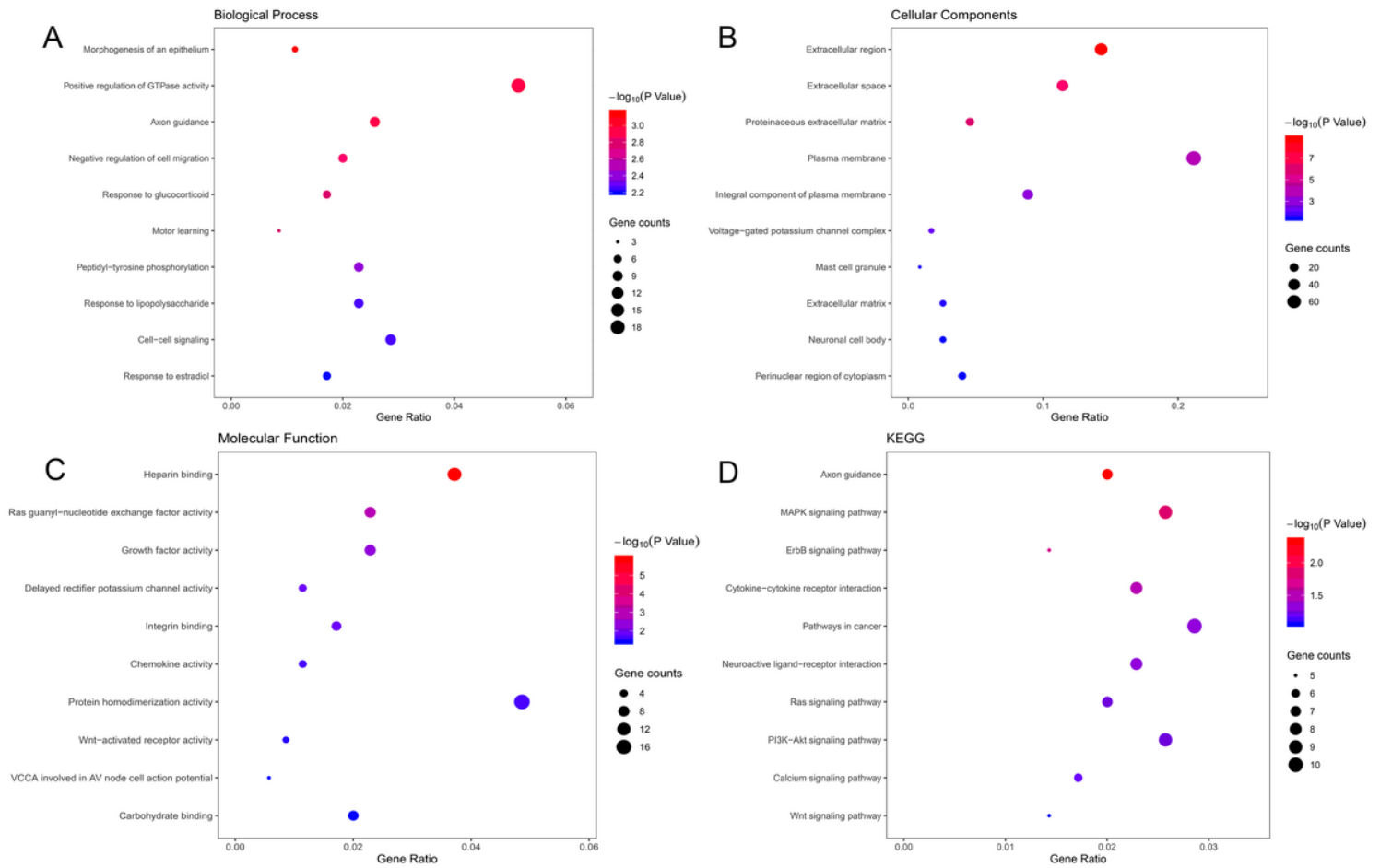


Figure 5

Functional enrichment analysis of DEGs in BMCs from Ho tissues demonstrated via bubble plot. (A) Top 10 intensively enriched biological processes in DEGs. (B) Top 10 intensively enriched cell component in DEGs. (C) Top 10 intensively enriched molecular function in DEGs. (D) Top 10 intensively enriched KEGG pathway in DEGs.

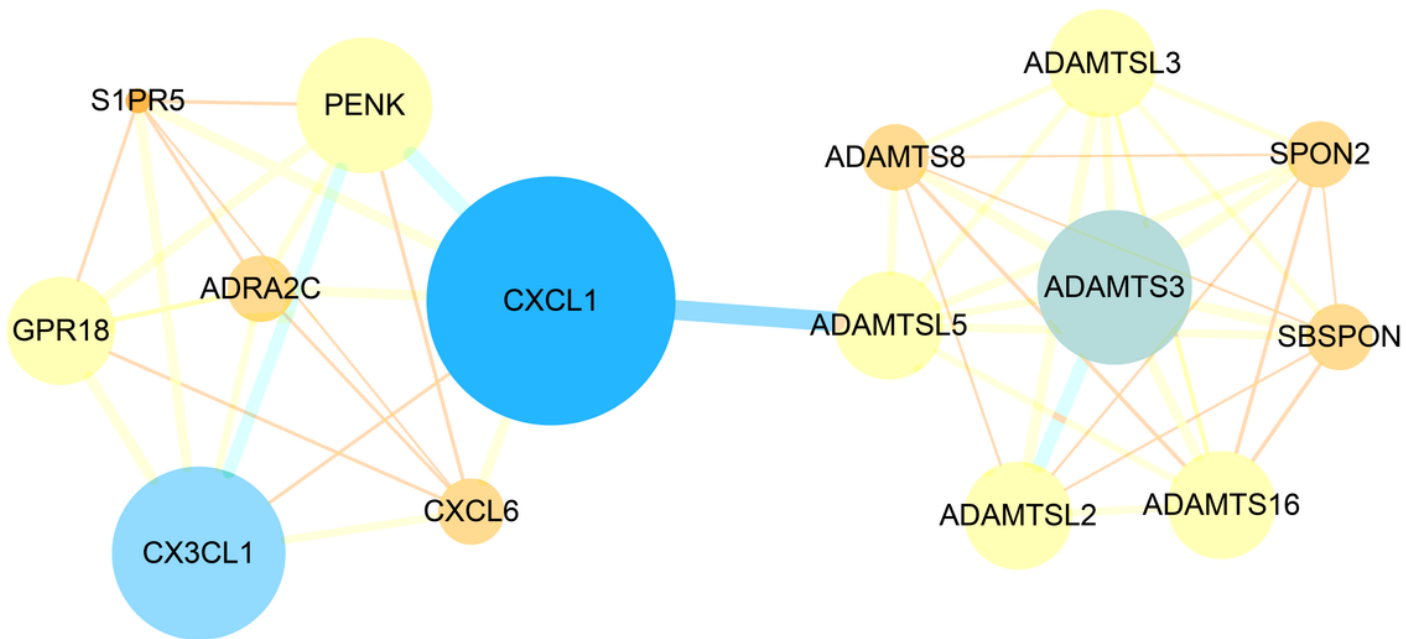


Figure 6

The most significant module was identified with 15 nodes and 50 edges. Small-sized or brightly colored circles and lines mean a lower value of combined score.

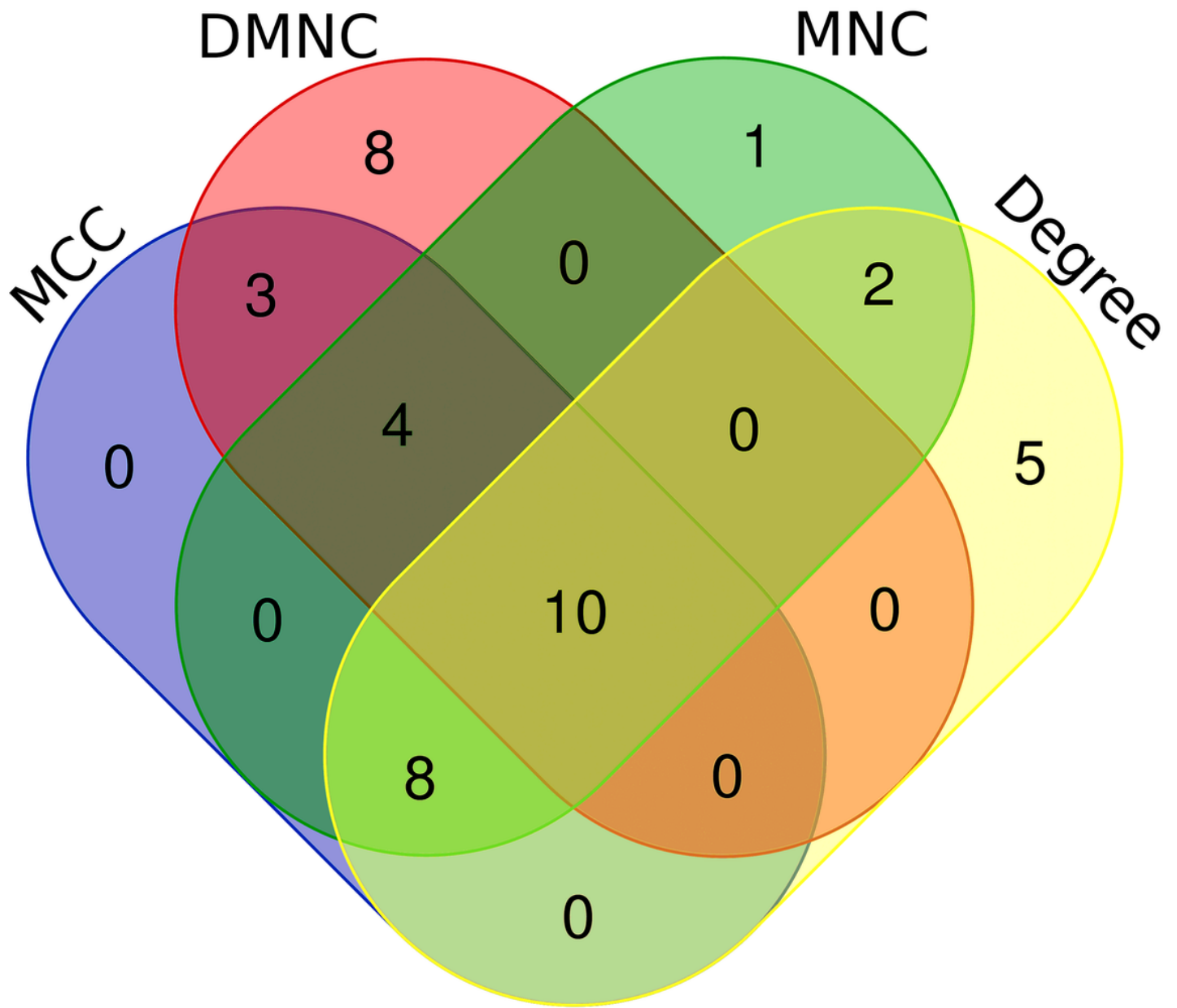


Figure 7

Hub genes identified via Venn diagram.